

Photoemission study of the electronic structure of Am, AmN, AmSb, and Am₂O₃ filmsT. Gouder,^{1,*} P. M. Oppeneer,² F. Huber,¹ F. Wastin,¹ and J. Rebizant¹¹*European Commission, Joint Research Centre, Institute for Transuranium Elements, Postfach 2340, D-76125 Karlsruhe, Germany*²*Department of Physics, Uppsala University, Box 530, S-751 21 Uppsala, Sweden*

(Received 1 February 2005; revised manuscript received 28 June 2005; published 28 September 2005)

Thin films of Am, AmN, AmSb, and Am₂O₃ have been prepared by sputter deposition. Their electronic structures have been studied by x-ray and ultraviolet photoelectron spectroscopy (XPS and UPS, respectively). Care has been taken to achieve high-purity Am films. While the Am UPS spectrum reveals the presence of a conduction band, practically no such signature appears in the spectra of AmN, AmSb, and Am₂O₃, categorizing the later compounds as semiconductors or insulators. We present a consistent explanation of the peak structures in both the 5*f* valence-band and 4*f* core-level spectra in terms of final-state screening channels. In all four Am systems, we find the 5*f* electrons to be largely localized. The XPS core-level spectrum of Am metal indicates some residual 5*f* hybridization, which is substantially suppressed in AmN, AmSb, and Am₂O₃. We observe nearly no difference between the AmN and AmSb and Am₂O₃ spectra suggesting a similar 5*f* configuration, even though, in general, nitrides and antimonides are more covalent than oxides. The measured photoemission spectra are consistent with a 5*f*⁶ ground-state configuration for all four systems.

DOI: [10.1103/PhysRevB.72.115122](https://doi.org/10.1103/PhysRevB.72.115122)

PACS number(s): 71.20.Gj, 71.28.+d

I. INTRODUCTION

Americium is the first actinide element, where in the elemental form the 5*f* states appear to be localized, contrary to all earlier actinides (Th, Pa, U, Np, Pu) having itinerant *f* states. From the evolution of the equilibrium lattice parameters within the actinide series the itinerant-localized transition is known to take place between Pu and Am.^{1,2} Localization, i.e., retraction from bonding, results in a sudden increase in the lattice constant between Pu and Am, causing the density to drop by almost 40%. In the early actinides there is sufficient *f*-*f* orbital overlap to ensure formation of an itinerant *f* band. The orbital contraction with increasing nuclear charge (due to the lack of screening) leads to a reduced overlap and eventually to *f* localization. The *f* states in Am are situated close to the border of the intriguing localization (or, sometimes called Mott) transition, which makes their behavior particularly interesting. Indeed, it was shown that the Am-5*f* states are only weakly localized and at increased pressure, the 5*f* states become itinerant again.³⁻⁶

So far, most investigations concentrated on Am metal. Its electronic structure was studied by UPS, providing evidence for 5*f* localization.⁷ Much less is known about the behavior of Am-5*f* states in Am compounds. So far only a few Am chalcogenides and pnictides,⁸⁻¹² Am dioxide (AmO₂), Am sesquioxide (Am₂O₃), some Am Laves phases,¹³ and Am dihydride¹⁴ were prepared, but except for the americium oxides and hydrides, for which photoemission experiments were performed,¹⁴⁻¹⁶ no electronic structure investigations have been carried out. In Am compounds, modifications in the chemical environment, e.g., through a hybridizing ligand, might push the 5*f* states into itinerancy. Such a scenario was proposed for AmTe, which was predicted to be a heavy fermion with a narrow band of partial 5*f* character.¹⁷ Recent high-pressure experiments on AmTe revealed a sudden volume contraction, which could be related to a modification of the 5*f* states.¹⁸

In this paper, we report an electronic structure investigation of Am metal, AmN, AmSb, and Am₂O₃. Am samples have been prepared as thin films by sputter deposition. Subsequently, core-level XPS and valence-band UPS spectra have been measured. Earlier valence-band photoemission data⁷ confirmed 5*f* localization in Am metal: the 5*f* states are withdrawn from the Fermi level (E_F) and form a broad peak structure, of which the exact nature is still a matter of debate and will be addressed in this paper. Bulk Am metal was proposed to have localized *f* states in a ($J=0$) 5*f*⁶ configuration, consistent with the absence of magnetic order. The Am sample used, however, contained a large fraction of residual Al (30%); therefore, it can be questioned if the measured photoemission spectrum is intrinsic to Am, which could have possible consequences for its interpretation. Our spectra, measured on high-purity Am, do not show significant differences with respect to the earlier measurements, thus, confirming the proposed picture of localized 5*f*s in Am metal. Also for Am₂O₃ we observe, as one would expect, localized 5*f* states in a 5*f*⁶ configuration of trivalent Am. The valence-band spectra of AmN and AmSb bear particular importance for an emerging picture of the electronic structure of the Am monpnictides. Recently, electronic structure calculations were performed for the Am monpnictides, using the self-interaction corrected local spin-density approximation (SIC-LSDA).¹⁹ These calculations predict a huge *f* partial density of states (DOS) at E_F throughout the Am monpnictide series, rendering the Am monpnictides to be metallic rocksalt compounds with a very high specific heat coefficient. As will be discussed, a rather different picture of the electronic structure emerges from our study and from the related theoretical²⁰ paper which follows this one.

In Sec. II, we first outline the experimental technique and subsequently present our results in Sec. III. An emerging picture of the electronic structures of Am and the Am compounds is presented in Sec. IV, and our conclusions are formulated in Sec. V.

II. EXPERIMENTAL DETAILS

High-purity thin films of Am have been prepared *in situ* by dc sputtering in an Ar atmosphere (2–20 Pa, Ar, Am target at -700 V). The plasma in the diode source was maintained by injection of electrons of 50 to 100 eV energy. As sputter gas, we used ultrahigh purity Ar (99.9999%). The deposition rate was about one monolayer per second and the film thickness ranged from 80 to 120 atomic layers. To prevent overheating, the Am target was gas cooled. The substrate was also kept at room temperature. The Am target was cleaned before introduction into the vacuum chamber by mechanical polishing. The background pressure of the plasma chamber was 4×10^{-7} Pa. For the spectroscopic experiments, we used a single crystalline Mo (100) substrate, which was cleaned *in situ* by Ar ion sputtering at $T=673$ K. The deposition currents were typically 1–2 mA.

Using a similar setup, AmN films were prepared by reactive sputter deposition from the Am metal target in an Ar atmosphere containing a nitrogen (N_2) admixture. The nitrogen content of the films depended on the partial N_2 pressure, but saturated at high N_2 pressure at a N/Am atomic ratio of 1. This is due to the rare-earth-like reactivity (trivalence) of Am. Already Pu shows no tendency of forming higher nitrides,²¹ while U (Ref. 22) and Th (Ref. 23) do. The composition of the films was deduced from the N-1s/Am-4f intensity ratio. Am₂O₃ was prepared by reactive sputtering in an Ar-O₂ mixture. Formation of the sesquioxide was confirmed by the O-1s/Am-4f ratio. It takes place in a wide O₂ pressure range, and only at high O₂ pressure AmO₂ forms. AmSb in turn, was prepared by codeposition of Am and Sb from the metallic targets. The film composition was adjusted by varying the deposition rates (by setting the respective target voltages). The film composition was obtained from the Sb-3d/Am-4f ratio.

Photoelectron spectra were recorded using a Leybold LHS-10 hemispherical analyzer. XPS spectra were taken using Al-K_α (1486.6 eV) radiation with an approximate resolution of 1 eV. UPS measurements were made using He I and He II ($h\nu=21.22$ eV and 40.81 eV, respectively) excitation produced by a high-density plasma UV source (SPECS). The total resolution in UPS was 0.1 to 0.05 eV for the high-resolution scans. The background pressure in the analysis chamber was better than 10^{-8} Pa.

III. RESULTS

A. Valence-band study of Am

Figure 1 shows the He I and He II valence-band spectra measured on an Am metal film. The spectra obtained for pure Am metals are consistent with the earlier published spectra,⁷ which were also obtained on an evaporated Am metal specimen with an initial thickness of about 2 μm containing, however, a substantial presence of Al (30%). In principle, the corresponding dilution of the Am could press the 5f's toward localization, however, comparing it to our spectra obtained for pure Am (Fig. 1), we do not observe significant differences. The Al *p* states are broad and, since their cross section for high-energy radiation is small, the dominating peaks are *f*

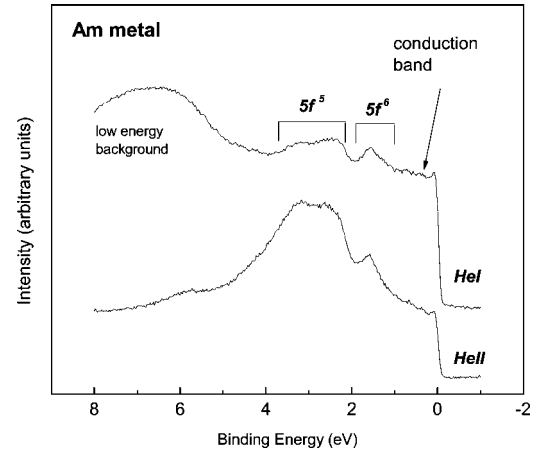


FIG. 1. He I and He II spectra measured on a high-purity Am metal film.

electron related. The peak structures are better resolved in our spectrum due to the higher instrumental resolution. The spectrum of pure Am shows a density of states at the Fermi level, which is in agreement with its metallic nature. The most prominent feature in the He II spectrum is the large peak structure extending from 1 to 4 eV binding energy. From a cross-section consideration,⁷ it was concluded that the peak must be due to 5*f* states. In contrast to early actinides, the Am-5*f* states are not pinned at the Fermi level, but they are shifted to higher-binding energy. This provides clear evidence for 5*f* localization, very similar to what is found for the rare earths, where the 4*f*s, too, are observed at higher binding energies.²⁶ Despite the fact that photoemission from localized levels must give final-state multiplets, no simple correspondence with one such multiplet could be found. An explanation can be given in terms of two coexisting final states with the corresponding multiplet structures.²⁸ Emission of an *f* electron from the 5*f*⁶ ground-state configuration leaves an *f* hole behind, which can be screened either by a supplementary *f* state (5*f*⁵-*f*=5*f*⁶) or by a *d* state (5*f*⁵-*d*). Thus, we have the following two final-state channels:

$$5f^6 \Rightarrow [5f^5]^* \begin{cases} [5f^5]_f = 5f^6 & (\text{good screening}) \\ [5f^5]_d = 5f^5 & (\text{poor screening}). \end{cases} \quad (1)$$

The *f*-screened final state appears at lower-binding energy (good screening), the *d*-screened final state appears at higher binding energy. In this way, two different 5*f* configurations, namely 5*f*⁵ and 5*f*⁶ appear as results of photoemission from the single 5*f*⁶ ground state. In this scenario, the main peak system between 2 and 4 eV represents the poorly screened 5*f*⁵ final state and the small peak at 1.8 eV represents the well-screened 5*f*⁶. The peak shapes are well consistent with the 5*f*⁵ and 5*f*⁶ final state multiplet structures.^{28,29} The apparently poor resolution of the multiplets (the different terms cannot be distinguished) is not surprising. Similar resolutions are observed for the rare earths,³⁰ and they can be attributed mainly to lifetime effects.³¹

Generally, such competing final states occur in weakly hybridized systems, where the good-screening channel closes once the screening states become localized. Then the alternative screening channel, poor screening, becomes dominant. So the ratio of the two final-state peaks gives an indication for the hybridization strength. In the He I spectrum (Fig. 1), the $5f^5$ intensity is comparable to the $5f^6$ intensity, but in the He II spectrum it is considerably reduced. There are two possible explanations: (i) either this signal contains appreciable d character (compared to the f cross section, the d cross sections is weaker for He II radiation)—but this seems improbable because a multiplet is an atomic feature and, as such, no hybridization takes place—and a mere superposition of two independent signals (f multiplet and d band) would not give such a well-defined peak. Instead, we think (ii) that the reduction is caused by a surface effect. For atoms at or near the surface, the weak hybridization of the f states is suppressed because of the lowered coordination. Consequently, the well-screened final state, which is related to the f hybridization, is reduced. Since the He II excited spectra are more surface sensitive than He I (the mean free path is about 50% of the one for He I),²⁷ the well-screened peak is suppressed. Quite importantly, such evolution of intensities excludes an alternative explanation,²⁸ based on the coexistence of $5f^6$ and $5f^5$ signals caused by a heterogeneous mixed-valence state. In this proposal, Am would have at its surface a divalent configuration (Am $5f^7$), whereas Am atoms in the bulk would have the conventional trivalent Am- $5f^6$ configuration. In this heterogeneous mixed state, the surface atoms were proposed to lead to the $5f^6$ final-state peak and the Am bulk atoms would give the $5f^5$ final state. If this was the case, the more surface-sensitive He II UPS should show an increased $5f^6$ signal, but exactly the opposite is observed. Therefore, we conclude, rather, that this peak corresponds to the well-screened bulk final state, which means that the hybridization cannot be neglected. The possibility that the peak at 1.8 eV could be due to different screening channels was considered in Ref. 28 too, but the divalent surface-state explanation was preferred. The explanation of the UPS spectrum in terms of heterogeneous divalent-trivalent contributions was also criticized by Cox, Ward, and Haire (Ref. 14), who performed high-energy photoemission experiments on Am metal, utilizing a variable-takeoff angle.

B. Valence-band study of Am₂O₃

In the Am₂O₃ spectrum (see Fig. 2), the conduction band has disappeared as is exemplified by the zero intensity at the Fermi level. This finding is consistent with the nonmetallic character of Am₂O₃. The three s - d electrons in the Am conduction band are transferred into the O- $2p$ valence band, which is located between 4 and 6 eV binding energy. The peak at 2 eV is attributed to Am- $5f$ states, because it shows the typical f -like enhancement in the He II spectrum. In contrast to Am metal, there is only one final state. Because Am₂O₃ has also a $5f^6$ ground-state configuration, and only the poorly screened ($5f^5$) final state is expected, this peak must correspond to the $5f^5$ final-state configuration. The emission at 3–7 eV is due to the O- $2p$ emission, as in other

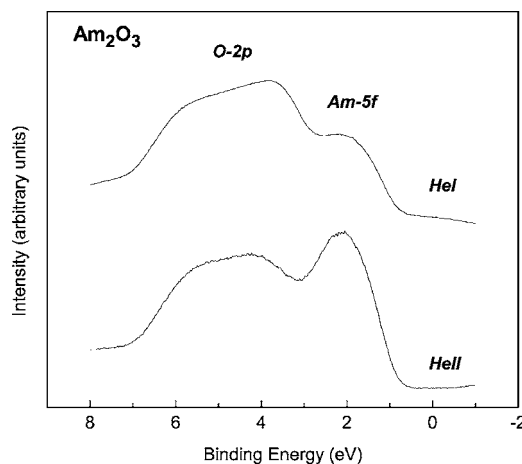


FIG. 2. He I and He II spectra obtained for an Am₂O₃ film.

actinide oxides. Its enhancement in the He I spectrum is fully consistent with the increased p cross section.

The $5f^5$ peak in Am₂O₃ does not shift to higher-binding energy as compared to Am metal. This seems surprising when considering that the Am-O bond in Am₂O₃ has ionic character. Even though, in general, the binding energy increases with the oxidation state (less screening electrons, higher electrostatic potential, etc.), additional factors (Madelung energy, shift of Fermi energy, etc.) may upset or even reverse this rule. The considerable high-binding energy shift upon oxidation, observed for early actinides (U, Np, and Pu), is mainly due to the change of the screening mechanism from well (f) to poor (d) type, when the $5f$ states change from itinerant (metal) to localization (oxide). In Am, however, the $5f$ states are already quite localized in the metal, and consequently there is no significant change in screening type and this cause for the high-binding energy shift falls away.

C. Valence-band study of AmN and AmSb

The valence-band spectrum of AmN (Fig. 3) shows one broad, unresolved peak ranging from 1 to 5 eV binding energy. Its shape is different in the He I and He II spectra, indicating that this peak is composed of several components (N- $2p$ and Am- $5f$) with different cross-section behavior. The components can be separated by subtracting the He I spectrum—which is primarily sensitive to N- $2p$ emission—from the He II spectrum, where the $5f$ signal dominates.³² The result is qualitatively shown in Fig. 3, with some small uncertainty remaining concerning the intensity normalization. The N- $2p$ peak is located at 4 eV binding energy, where it has also been observed in other actinide nitrides (e.g., ThN, UN).^{22,23} It extends to the lower binding energy and it is not clear whether this is due to some remaining f intensity, or whether the p band extends to these energies. The Am- $5f$ peak appears at 2–3 eV binding energy, which is slightly higher than for the oxide. Furthermore, the absence of any local magnetic moment in AmN (Ref. 33) and AmSb (Ref. 9), in spite of $5f$ localization, is consistent with a ($J=0$) $5f^6$ ground-state configuration. In contrast to Am metal, there is

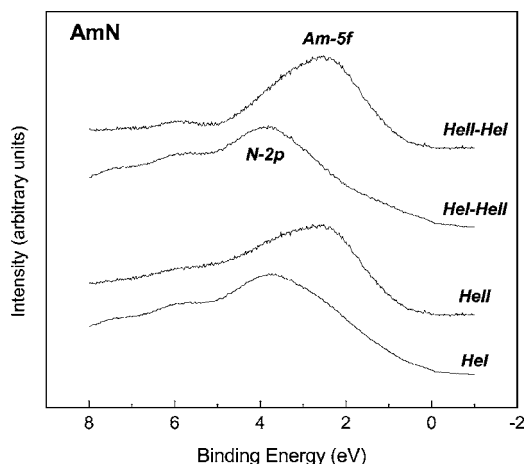


FIG. 3. He I and He II spectra measured on an AmN film. The N-2*p* anion band partially overlaps with the 5*f* multiplet. The contributions due to the *f* and *p* signals are separated in the difference spectra.

only one peak—thus, only one final state. Because the 5*f* states in the nitride are expected to be less hybridized than in the metal (see below), it is attributed to the 5*f*⁵ rather than the 5*f*⁶ final state. The AmN valence-band spectrum reveals no emission at *E*_F, but there is a constantly decreasing intensity, reaching zero shortly before *E*_F. We conclude that AmN is a small band-gap insulator.

The 5*f*⁵ peak of AmN is considerably broader than that of Am₂O₃ or Am metal. This cannot be explained by conventional broadening mechanisms such as charge or phonon broadening, which occur in insulators, because in Am₂O₃, which is also an insulator, there is no broadening. We instead attribute it to a lifetime effect. The 5*f* final state has a short lifetime, because it superimposes energetically with the N-2*p* band, and thus filling of the *f* hole would occur faster.³¹ The O-2*p* band, on the other side, lies at higher-binding energy, so that charge transfer into the 5*f* hole is energetically unfavorable and in addition there is less hybridization.

The valence-band UPS spectrum of AmSb is shown in Fig. 4. As expected, the photoemission spectrum of AmSb is similar to that of AmN. The Sb-4*p* and Am-5*f* contributions were separated by subtracting the He I and He II spectra. The main 5*f* response occurs at practically the same high-binding energy and the well-screened *f* peak at low-binding energy (5*f*⁶ final state) is missing. However, a noticeable difference is that AmSb shows a small DOS at the Fermi level, which is more pronounced in the He I than He II spectrum. It is attributed to the Sb-5*p*- and Am-7*s6d*-derived band, which would extend up to *E*_F. AmSb would thus possibly not be an insulator, although it could exhibit pseudogap behavior. Another explanation could be that there is a residual content of Am or Sb metal in the sample and the observed intensity could be due to their conduction bands. To exclude this possibility, we have carried out experiments on different compositions from Am_{0.3}Sb_{0.7} to Am_{0.8}Sb_{0.2}. In all cases, we observed the small intensity at *E*_F, which passes through a minimum around Am_{0.5}Sb_{0.5}. Thus, while inhomogeneity of the prepared AmSb films cannot fully be excluded, we are rather inclined to attribute the residual DOS to a valence band extending up to *E*_F.

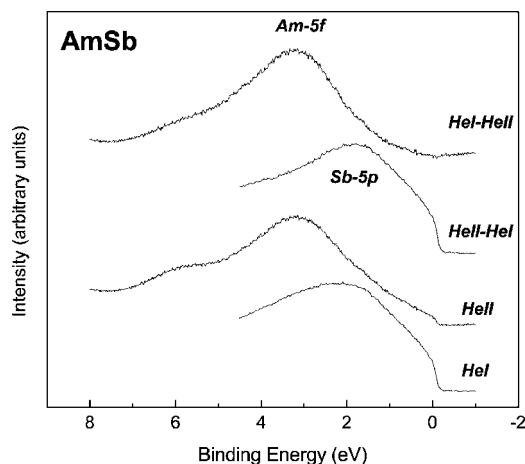


FIG. 4. He I and He II spectra measured on AmSb. The Sb-5*p* anion band partially overlaps with the 5*f* response. The *f*-related and *p*-related signals are separated in the difference spectra.

D. Core-level study of Am, AmN, AmSb, and Am₂O₃

Figure 5 compares the Am-4*f* core-level spectra of Am, Am₂O₃, AmN, and AmSb. The Am and Am₂O₃ spectra are consistent with previously published data.^{7,16} All spectra show the spin-orbit split 4*f*_{7/2} and 4*f*_{5/2} peaks around 449 and 463 eV binding energy, respectively. In Am metal, the main lines are accompanied by a satellite at 3 eV lower-binding energy. Again, as for the UPS valence-band spectra, the interpretation is conceived in terms of final-state screening. The low-binding energy satellite corresponds to the well- (*f*-) screened final state, thus pointing to residual hybridization of the *f* states with the conduction band. The main peak corresponds to the poorly (*d*-) screened final state. In itinerant (hybridized) systems, the well-screened peak dominates (U, Np, Pu); while in localized systems the poorly screened peak is strong (UPd₃, for example).³⁴ The predominance of the poorly screened peak in Am, thus, exemplifies 5*f* localization, while the still observable well-screened peak points to some residual hybridization of the 5*f* states with the

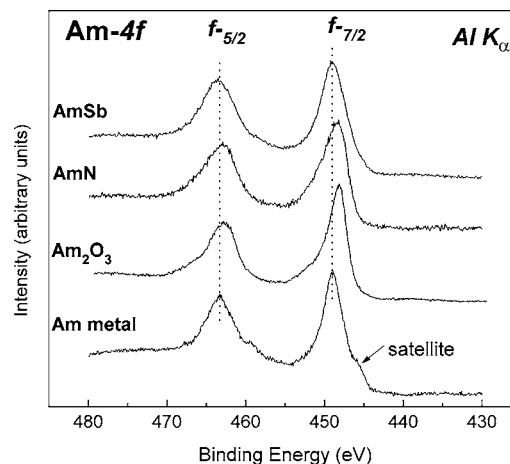


FIG. 5. Am-4*f* core-level spectra of Am, AmN, AmSb, and Am₂O₃. The size of the well-screened satellite shoulder demonstrates that the 5*f* hybridization is most pronounced in Am metal.

TABLE I. Core-level binding energies for the different Am compounds.

Compound	Am- $4f_{7/2}$	Ligand core-level
Am metal	449.0 eV	—
Am ₂ O ₃	448.2 eV	O-1s: 529.0 eV
AmN	448.3 eV	N-1s: 396.1 eV
AmSb	448.9 eV	Sb-3d: 527.6 eV

conduction band being present. Both the $4f$ and $5f$ peaks contain the well-screened and poorly screened component. But it is interesting to notice that the well-screened peak in the $4f$ spectrum is significantly weaker than that in the corresponding He I excited $5f$ spectrum. This cannot be due to a surface effect, because the information depths in XPS and He I UPS are similar. Instead, we assume that the final state after ejection of a $4f$ electron is more localized than after ejection of a $5f$ electron, because the increase of the core potential is more pronounced: the inner ($4f$) electrons screen the nuclear charge more efficiently than the outer ($5f$) states similar to Am metal. The Am- $4f_{7/2}$ core-level binding energies of the respective Am compounds are listed in Table I, as are the principal ligand core-level energies.

In Am₂O₃, AmN, and AmSb, only single spin-orbit split components are observed. There is no coexistence of well-screened and poorly screened peaks anymore. It is obvious that it can only be the poorly screened peak which remains. Otherwise, it would imply that, e.g., AmN is such an itinerant system that the well-screened peak completely dominates. In this case, AmN should be more itinerant than α -Pu. Clearly, this is not the case as is shown by the lattice constant¹² and the UPS spectrum. The disappearance of the well-screened peak shows the $5f$ states to be less hybridized in the compounds than in the Am metal.

IV. DISCUSSION

A. Electronic structure picture

Our UPS spectra prove AmN to be a small-gap insulator. Recently, a theoretical study proposed an electronic structure picture of the Am mononictides on the basis of SIC-LSDA calculations.¹⁹ These calculations predict for all the Am mononictides a huge $5f$ partial DOS at the Fermi level. In the SIC-LSDA picture, the Am mononictides would be metallic, possibly heavy-fermion materials, exhibiting a large specific-heat coefficient on account of the hybridized, narrow $5f$ band at E_F . AmN was indeed shown to be a temperature-independent paramagnet (TIP) with a very high paramagnetic susceptibility ($\chi_0 = 777 \times 10^{-6}$ emu/mol).³³ The theoretical picture of a huge $5f$ partial DOS at E_F appeared to confirm the very high χ , when one assumes Pauli paramagnetism.¹⁹ However, we cannot observe any high DOS near E_F in the UPS photoemission spectrum, which definitely eliminates the high $5f$ -DOS electronic structure model. On the contrary, in more recent calculations employing the local-density approximation (LDA) scheme, the LDA+ U scheme, as well as the f -core scheme, Ghosh *et al.*

(Ref. 20) arrived at a quite different electronic structure picture: these three electronic structure approaches all predict the Am mononictides to be either narrow-gap semiconductors or pseudogap materials. The LDA+ U approach would, in addition, provide good values for the equilibrium lattice parameters and the binding energy of the Am- $5f$ states. Since in these approaches, there is at the most a small DOS at E_F , the high-magnetic susceptibility cannot be explained thereby. However, the large-magnetic susceptibility could alternatively be explained by Van Vleck paramagnetism, which can occur when there is a small or moderate energy gap between a $J=0$ ground state and higher-lying excited states. The possibility of a $J=0$ ground state giving rise to Van Vleck paramagnetism was previously suggested for Am metal, too.³⁵ A similar explanation was also proposed³⁶ for the Pu monochalcogenides, which exhibit TIP with very high susceptibility values (e.g., see Refs. 17 and 37). Estimations²⁰ of the Am mononictide susceptibility based on the Van Vleck mechanism provides values for χ_0 which are of the order of magnitude of the available experimental data.^{9,33,38} Thus, we arrive at an electronic structure picture for the Am mononictides, essentially being semiconducting or pseudogap materials, which is consistent with the photoemission and susceptibility data.

B. $5f$ itinerancy and ground-state configuration

When comparing Am and its three compounds, the well-screened Am- $4f$ peak disappears in the XPS spectra together with the $5f^6$ final-state component in the UPS spectra. This points to a common origin of the two. For the core-level, final-state screening effects are responsible for the change. It is reasonable to conclude that similar screening effects account for the change in the valence spectra. Above it was explained that the $5f^6$ emission is either due to a surface component of divalent Am (i.e., $5f^7 \rightarrow 5f^6$ transition) or to the well-screened $5f$ final state ($5f^6 \rightarrow 5f^5 f^1$ transition). We favor here this second explanation and assign the $5f^6$ peak to the well-screened $5f^5 f^1$ final state, which does not come from a top surface layer with changed valence. Already the intensity evolution from the He I to He II spectra indicated that.

The residual hybridization in Am metal (well-screened final state) is further suppressed in AmN and AmSb, and, consequently, the $5f$ states are even more localized in AmN and AmSb than in Am metal. AmN and AmSb behave differently from AmTe, where, apparently, hybridization effects may lead to itinerancy of the $5f$ states under pressure.^{17,18} Instead AmN and AmSb are similar to Am₂O₃, which is an ionic system with little covalence. The magnetic behavior of AmN, which is a TIP, is consistent with a localized $5f^6$ configuration.

V. CONCLUSIONS

We have performed UPS and XPS photoelectron spectroscopy on high-purity Am metal films, as well as on thin films of AmN, AmSb, and Am₂O₃. Our spectroscopic study provides the first electronic structure results for AmN and AmSb.

Our investigation, carried out on high-purity Am films, permits a consistent interpretation of the f -related structures in the UPS valence-band spectrum. The peak at low-binding energy (1.8 eV) is attributed to the well-screened channel of photoemission out of the $5f^6$ ground state, whereas the broader peak at higher binding energy is attributed to the poor screening channel, rather than to a change in the Am surface configuration. Our assignment is in agreement with the outcome of another study on Am metal¹⁴ and it is supported by the spectra measured for Am₂O₃, AmN, and AmSb, in which the well-screened peak is suppressed.

The $5f$ electrons in AmN, AmSb, and Am₂O₃ are consequently even more localized than in Am metal. This is exemplified, too, by the decrease of the well-screened satellite in $4f$ photoemission spectra. In AmN and AmSb, Am is forced into a trivalent $5f^6$ configuration, consistent with the TIP susceptibility. The UPS valence-band spectra of the three Am compounds show no $5f$ -related response near the Fermi level and even no conduction band (i.e., AmN and Am₂O₃ exhibit loss of metallicity) or, at the most, a small valence intensity (AmSb). Thus, our study categorizes AmN and Am₂O₃ as insulators, while AmSb could be a quasigap material. The high $5f$ DOS at the Fermi energy as proposed by the SIC-LSDA approach¹⁹ for the Am mononictides is not confirmed by our photoemission results. An alternative elec-

tronic structure picture is offered by the LSDA+ U approach, which predicts the Am mononictides to be semiconductors or, depending on the value of the Coulomb U , quasigap materials, without any notable $5f$ partial DOS near E_F .²⁰ The observed high, temperature-independent paramagnetic susceptibility can be satisfactorily explained by a Van Vleck mechanism.

Am and AmN are close to the localization threshold on the localized side. Previous photoemission studies addressed the localization threshold from the delocalized side by investigating Pu and PuN.^{21,24,25} We note that in both cases, adding nitrogen pushes the $5f$ states into further localization. While in Pu there is a changeover from itinerancy to localization, in Am there is a further decrease of the $5f$ hybridization.

ACKNOWLEDGMENTS

We thank M. S. S. Brooks and G. H. Lander for helpful discussions. P.M.O. gratefully acknowledges financial support for access to the Actinide User Laboratory at the Institute for Transuranium Elements, Karlsruhe from the European Community Access to Research Infrastructure Programme under Grant No. HPRI-CT-2001-00118.

*Corresponding author. Electronic address: gouder@itu.fzk.de

¹S. S. Hecker and L. F. Timofeeva, *Los Alamos Sci.* **26**, 244 (2000).

²*Handbook on the Physics and Chemistry of the Actinides*, edited by A. J. Freeman and G. H. Lander (North-Holland, Amsterdam, 1984–1988), Vols. 1–5.

³R. B. Roof, R. G. Haire, D. Schiferl, E. A. Kmetko, and J. L. Smith, *Science* **207**, 1353 (1980).

⁴U. Benedict, J. P. Itié, C. Dufour, S. Dabos, and J. C. Spirlet, in *Americium and Curium Chemistry and Technology*, edited by N. Edelstein, J. D. Navratil, and W. W. Schulz (Reidel, Dordrecht, 1985), p. 213.

⁵S. Heathman, R. G. Haire, T. Le Bihan, A. Lindbaum, K. Litfin, Y. Méresse, and H. Libotte, *Phys. Rev. Lett.* **85**, 2961 (2000).

⁶J. C. Griveau, J. Rebizant, G. H. Lander, and G. Kotliar, *Phys. Rev. Lett.* **94**, 097002 (2005).

⁷J. R. Naegele, L. Manes, J. C. Spirlet, and W. Müller, *Phys. Rev. Lett.* **52**, 1834 (1984).

⁸A. W. Mitchell and D. J. Lam, *J. Nucl. Mater.* **37**, 349 (1970).

⁹B. D. Dunlap, D. J. Lam, G. M. Kalvius, and G. K. Shenoy, *J. Appl. Phys.* **42**, 1719 (1971).

¹⁰J. W. Roddy, *J. Inorg. Nucl. Chem.* **36**, 2531 (1974).

¹¹J. P. Charvillat, U. Benedict, D. Damien, C. H. de Novion, A. Wojakowski, and W. Müller, in *Transplutonium 1975*, edited by W. Müller and R. Lindner (North-Holland, Amsterdam, 1976), p. 79.

¹²F. Wastin, J. C. Spirlet, and J. Rebizant, *J. Alloys Compd.* **219**, 232 (1995).

¹³A. T. Aldred, B. D. Dunlap, D. J. Lam, and G. K. Shenoy, in *Transplutonium 1975*, edited by W. Müller and R. Lindner

(North-Holland, Amsterdam, 1976), p. 191.

¹⁴L. E. Cox, J. W. Ward, and R. G. Haire, *Phys. Rev. B* **45**, 13239 (1992).

¹⁵B. W. Veal, D. J. Lam, H. Diamond, and H. R. Hoekstra, *Phys. Rev. B* **15**, 2929 (1977).

¹⁶J. R. Naegele, J. Ghijsen, and L. Manes, in *Actinides—Chemistry and Physical Properties, Structure and Bonding 59/60*, edited by L. Manes (Springer, Berlin, 1985), p. 197.

¹⁷P. Wachter, M. Filzmoser, and J. Rebizant, *Physica B* **293**, 199 (2001).

¹⁸M. Idiri, Ph.D. thesis, University of Grenoble, 2003.

¹⁹L. Petit, A. Svane, W. M. Temmerman, and Z. Szotek, *Phys. Rev. B* **63**, 165107 (2001).

²⁰D. B. Ghosh, S. K. De, P. M. Oppeneer, and M. S. S. Brooks, following paper, *Phys. Rev. B* **72**, 115123 (2005).

²¹L. Havela, F. Wastin, J. Rebizant, and T. Gouder, *Phys. Rev. B* **68**, 085101 (2003).

²²L. Black, F. Miserque, T. Gouder, L. Havela, J. Rebizant, and F. Wastin, *J. Alloys Compd.* **315**, 36 (2001).

²³T. Gouder, L. Havela, L. Black, F. Wastin, J. Rebizant, P. Boulet, D. Bouëxière, S. Heathman, and M. Idiri, *J. Alloys Compd.* **336**, 73 (2002).

²⁴A. J. Arko, J. J. Joyce, L. Morales, J. Wills, J. Lashley, F. Wastin, and J. Rebizant, *Phys. Rev. B* **62**, 1773 (2000).

²⁵T. Gouder, L. Havela, F. Wastin, and J. Rebizant, *Europhys. Lett.* **55**, 705 (2001).

²⁶J. K. Lang, Y. Baer, and P. A. Cox, *J. Phys. F: Met. Phys.* **11**, 121 (1981).

²⁷M. P. Seah and W. A. Dench, *Surf. Interface Anal.* **1**, 2 (1979).

²⁸N. Mårtensson, B. Johansson, and J. R. Naegele, *Phys. Rev. B*

- 35**, 1437 (1987).
- ²⁹F. Gerken and S. Schmidt-May, *J. Phys. F: Met. Phys.* **13**, 1571 (1983).
- ³⁰J. N. Chazaviel, M. Campagna, G. K. Wertheim, and P. Y. Schmidt, *Solid State Commun.* **19**, 725 (1976).
- ³¹Y. Baer, R. Hauger, Ch. Zürcher, M. Campagna, and G. K. Wertheim, *Phys. Rev. B* **18**, 4433 (1978).
- ³²J. J. Yeh and I. Lindau, *At. Data Nucl. Data Tables* **32**, 1 (1985).
- ³³B. Kanellakopoulos, J. P. Charvillat, F. Maino, and W. Müller, in *Transplutonium 1975*, edited by W. Müller and R. Lindner (North-Holland, Amsterdam, 1976), p. 181.
- ³⁴Y. Baer, H. R. Ott, and K. Andres, *Solid State Commun.* **36**, 387 (1980).
- ³⁵D. B. McWhan, Ph.D. thesis, University of California, Berkeley, 1961 (UCRL Report No. 9695); D. B. McWhan, B. B. Cunningham, and J. C. Wallmann, *J. Inorg. Nucl. Chem.* **24**, 1025 (1962).
- ³⁶P. M. Oppeneer, T. Kraft, and M. S. S. Brooks, *Phys. Rev. B* **61**, 12825 (2000).
- ³⁷V. Ichas, J. C. Griveau, J. Rebizant, and J. C. Spirlet, *Phys. Rev. B* **63**, 045109 (2001).
- ³⁸O. Vogt, K. Mattenberger, J. Löhle, and J. Rebizant, *J. Alloys Compd.* **271-273**, 508 (1998).